ACS Combinatorial Science

Research Article

pubs.acs.org/acscombsci

Discovery of a Direct Ras Inhibitor by Screening a Combinatorial Library of Cell-Permeable Bicyclic Peptides

Thi B. Trinh,[†] Punit Upadhyaya,[†] Ziqing Qian, and Dehua Pei*

Department of Chemistry and Biochemistry, The Ohio State University, 484 West 12th Avenue, Columbus, Ohio 43210, United States

Supporting Information

ABSTRACT: Cyclic peptides have great potential as therapeutic agents and research tools. However, their applications against intracellular targets have been limited, because cyclic peptides are generally impermeable to the cell membrane. It was previously shown that fusion of cyclic peptides with a cyclic cell-penetrating peptide resulted in cell-permeable bicyclic peptides that are proteolytically stable and biologically active in cellular assays. In this work, we tested the generality of the bicyclic approach by synthesizing a combinatorial library of 5.7 × 10^6 bicyclic peptides featuring a degenerate sequence in the first ring and an invariant cell-penetrating peptide in the second ring. Screening of the library against oncoprotein K-Ras G12V followed by hit optimization produced a moderately potent and cell-permeable K-Ras inhibitor, which physically blocks the Ras-effector interactions in vitro, inhibits the signaling events downstream of Ras in cancer cells, and induces apoptosis of the cancer cells. Our approach should be generally applicable to developing cell-permeable bicyclic peptide inhibitors against other intracellular proteins.

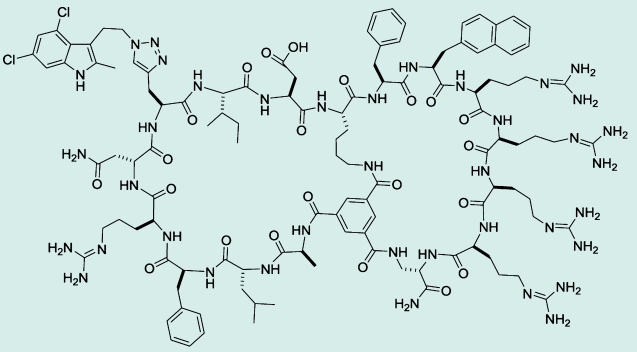

KEYWORDS: *anticancer agent, bicyclic peptide, cell-penetrating peptide, peptide library, Ras inhibitor*

INTRODUCTION

It is estimated that as much as 80% of all disease-relevant human proteins are beyond the reach of the two established classes of drugs, i.e., small-molecule and protein therapeutics.[1] Protein−protein interactions (PPIs), especially those that take place intracellularly, are the most notable examples of this "undruggable" class of targets.[2] Because PPIs typically involve large, flat binding sites, small molecules generally do not bind to the PPI interfaces with high affinity or specificity. While monoclonal antibodies can effectively block these PPIs, they are impermeable to the cell membrane. In recent years, there has been growing interest in developing structurally constrained peptides (e.g., cyclic and stapled peptides) as PPI inhibitors.[3,4] Unfortunately, cyclic peptides, like the proteins they are intended to mimic, are also generally impermeable to the cell membrane.

We recently discovered a small cyclic peptide, cyclo(FΦRRRRQ) (cFΦR_4, where Φ is L-2-naphthylalanine), as a powerful cell-penetrating peptide (CPP).[5−7] Mechanistic studies suggest that it binds directly to the phospholipids of the plasma membrane and is internalized by endocytosis.[7] Unlike most of the previously reported CPPs (e.g., Tat, penetratin, and nonaarginine), cFΦR_4 has the unusual ability to efficiently escape from the early endosome, giving rise to a cytosolic/nuclear delivery efficiency approximately an order of magnitude higher than that of the conventional CPPs.[6,7] Moreover, a number of biologically active cyclic peptides of varying sequences were effectively delivered into the cytosol of mammalian cells when fused with cFΦR_4 to form bicyclic peptides (bicyclic delivery).[7−9] The resulting bicyclic peptides were highly resistant to proteolysis and specifically inhibited the intended intracellular proteins in cultured mammalian cells. Encouraged by these results, we hypothesized that the bicyclic approach might provide a general solution for delivering biologically active cyclic peptides into mammalian cells. To test this hypothesis, we decided to generate a combinatorial library of bicyclic peptides, which contain the FΦR_4 motif in the first ring for cell entry and a degenerate peptide sequence in the second ring, to be screened for binding to a target protein of interest. We expected most (if not all) of the library members to be cell-permeable.

We chose one of the most challenging drug targets, the oncoprotein K-Ras, to test our method. K-Ras is a small GTPase that acts as a molecular switch during eukaryotic cell signaling.[10] In normal cells, K-Ras shuttles between an inactive GDP-bound state and an active GTP-bound state, a process regulated by guanosine nucleotide exchange factors (GEFs) and GTPase-activating proteins (GAPs). The Ras-GTP form physically interacts with and activates a multitude of effector proteins including kinases Raf and PI3K, ultimately leading to cell proliferation and survival. In cancer cells, K-Ras (also H-

Received: October 22, 2015
Published: December 8, 2015

DOI: 10.1021/acscombsci.5b00164
ACS Comb. Sci. 2016, 18, 75−85

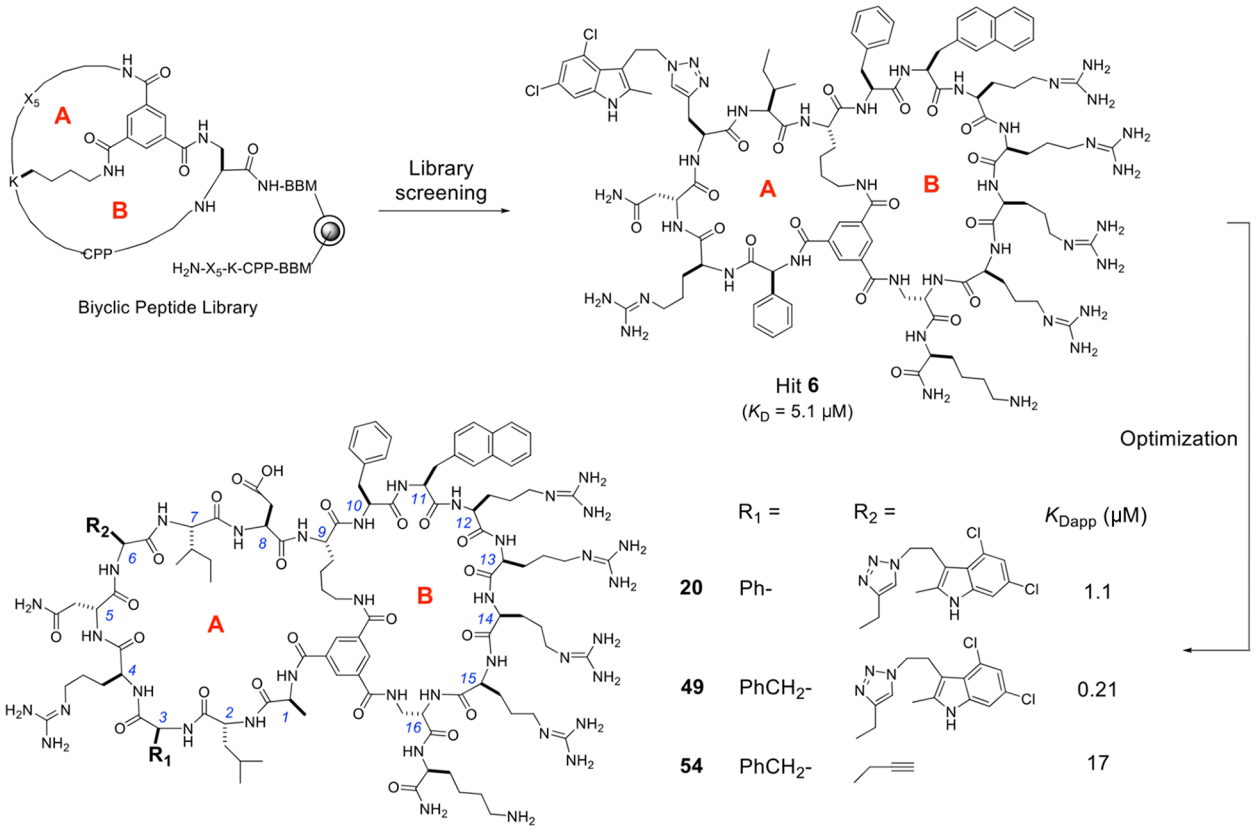

Figure 1. Flowchart showing the steps involved in the development of Ras inhibitors, which included design, synthesis, and screening of a bicyclic peptide library on spatially segregated TentaGel beads followed by hit optimization through medicinal chemistry approaches. CPP, FΦRRRR, or RRRRΦF. The amino acid residues in peptides **20**, **49**, and **54** are indicated by numbers in blue (1−16).

and N-Ras) is frequently mutated at codon 12 (e.g., G12V), 13, or 61; mutations at these positions abolish GAP-mediated GTP hydrolysis, rendering the mutant Ras constitutively active and causing uncontrolled cell growth. With mutations found in ∼30% of human cancers,[11] Ras is an attractive target for anticancer drug discovery. However, as a protein engaged in intracellular PPIs, Ras has been a very challenging target, described by some investigators as the "Holy Grail" or "Everest" of oncology targets.[12,13] Despite decades of intense efforts, no Ras inhibitor has advanced into the clinic. Only over the past few years have small-molecule and peptide inhibitors against Ras emerged.[14−16] Most of the reported Ras inhibitors target the membrane anchoring of Ras[14−17] or the nucleotide exchange activity of Ras,[18−25] while only a few interfere with the Ras-effector interactions.[21,26−30] In this work, screening of the bicyclic peptide library against the G12V mutant K-Ras and hit optimization resulted in a cell-permeable K-Ras inhibitor that physically blocks the Ras-effector interactions. Importantly, all of the bicyclic peptides tested in this study were cell permeable, strongly suggesting that incorporation of the $F\Phi R_4$ motif into one of the rings represents a general approach to the development of cell-permeable bicyclic peptide inhibitors against intracellular proteins.

RESULTS

Bicyclic Peptide Library Design. To obtain cell-permeable Ras inhibitors, we designed a bicyclic peptide library[31] featuring five degenerate residues (X_5) in the first ring (A ring) and a CPP motif in two orientations ($F\Phi R_4$ or $R_4\Phi F$) in the second ring (B ring): bicyclo[Tm-X_5-K-(CPP)-J]-BBM-resin, where B is β-alanine, J is L-2,3-diaminopropionic acid (Dap), and Tm is trimesoyl group (Figure 1). Each degenerate position (X^1−X^5) was constructed with a 26-amino acid set that included 10 proteinogenic L-amino acids (Ala, Asp, Gly, His, Ile, Gln, Arg, Ser, Trp, and Tyr), six unnatural L-amino acids [L-2-aminobutyric acid (Abu), L-norleucine (Nle), L-2-phenylglycine (Phg), L-4-fluorophenylalanine (Fpa), L-ornithine (Orn), and L-propargylglycine (Pra)], and 10 α-D-amino acids [ala, glu, phe, lys, leu, asn, pro, thr, naphthylalanine (nal), and val]. To increase the stringency of library screening, the Pra content on each bead was reduced 10-fold by using a 1:9 (mol/mol) mixture of Fmoc-Pra-OH and Fmoc-Lys(Ac)-OH during the coupling reaction for Pra.[32] Finally, to increase the binding affinity of the library compounds to K-Ras, we converted 4,6-dichloro-2-methyl-3-aminoethylindole (DCAI), a small molecule that binds K-Ras near the effector-binding site (K_D ∼ 1.1 mM),[19] into the corresponding azide and coupled it to the Pra residues through click chemistry.[33,34] The library (theoretical diversity 2.4×10^7) was synthesized on 2.0 g of 90-μm spatially segregated TentaGel resin (∼5.7×10^6 beads),[35,36] with each bead displaying a unique bicyclic peptide on its surface and a linear peptide of the same sequence inside the bead as an encoding tag. The detailed procedure of library synthesis is described in the Experimental Section and Scheme S1 of Supporting Information.

Library Screening. The bicyclic peptide library was screened against a biotinylated K-Ras G12V using an on-bead enzyme-linked assay. Binding of K-Ras to positive beads recruited a streptavidin-alkaline phosphatase conjugate (SA-AP) to the bead surface. Subsequent incubation in a solution of

DOI: 10.1021/acscombsci.5b00164
ACS Comb. Sci. 2016, 18, 75−85

5-bromo-4-chloro-3-indolyl phosphate (BCIP) produced a turquoise color on the positive beads. Screening a portion of the bicyclic peptide library (100 mg, ~300 000 beads) produced 21 intensely colored beads, which were isolated manually with a micropipet under a dissecting microscope and individually sequenced by the partial Edman degradation-mass spectrometry (PED-MS) method[37] to give 13 complete sequences (Table 1). With the exception of hit 5 (which has

Table 1. Hit Sequences from Peptide Library Screening[a]

hit	X^1	X^2	X^3	X^4	X^5
1	Arg	phe	Z	Z	phe
2[b]	Arg	Asp	Phg	Z	asn
3	Z	Z	pro	Gly	Ala
4	Z	Z	Ala	Ser	Ala
5	Z	Z	leu	pro	thr
6[b]	Phg	Arg	asn	Z	Ile
7	Z	thr	glu	Ala	asn
8	Z	nal	val	Gly	Gln
9	Z	Phg	Ser	Z	Z
10	Z	Phg	Nle	Ser	Z
11	Z	Ser	Nle	Z	Gly
12[b]	Z	Ser	Phg	Z	Z
13[b]	Z	Arg	val	Asp	Ala

[a]Z, 1:9 mixture of Pra and Lys(Ac). [b]Hits selected for resynthesis and solution-phase binding analysis.

$R_4\Phi F$ as the CPP motif), all of the other peptides (12 sequences) contained $F\Phi R_4$ in the B ring, suggesting that the CPP motif may also interact with the Ras protein surface. Hits **2**, **6** (Figure 1), and **13**, which each contain a single Pra/Lys(Ac) residue, were resynthesized with a Pra residue, derivatized with DCAI, and labeled with fluorescein isothiocyanate (FITC) at a C-terminal lysine side chain. Hit **12**, which has three Pra/Lys(Ac) residues, was resynthesized with a Pra-DCAI at the first position [based on the fact that most of the hits contained a Pra/Lys(Ac) at this position] and Lys(Ac) at the other two positions. In-solution binding analysis by fluorescence anisotropy (FA) revealed that hits **6**, **12**, and **13** bind to K-Ras G12V with apparent K_D values of 5.1, 20, and 9.0 μM, respectively, whereas hit **2** has no significant binding (Table 2). As expected, all four hit peptides are cell permeable, having cellular uptake efficiencies 25−56% that of $cF\Phi R_4$ (Figure S1). The lower uptake efficiency of the bicyclic peptides (relative to $cF\Phi R_4$) is likely due to their larger CPP ring size (equivalent to a cycloundecapeptide) and poorer binding to membrane phospholipids during endocytosis.[5]

Hit Optimization. Owing to its relatively high potency, hit **6** was selected for optimization. We first tested whether the size of the A ring could be expanded to generate additional sites for structural diversification. Although insertion of a single Ala either before or after the Phg-Arg-asn-Pra-Ile motif had minimal effect, simultaneous addition of two Ala residues N-terminal and one Ala C-terminal to the pentapeptide increased the binding affinity by ~5-fold (Table 2, K_{Dapp} = 1.2 μM for peptide **17**). Next, the three Ala residues were replaced with the 25 amino acids described above (except for Pra) to generate a second-generation library, bicyclo[Tm(X-X-Phg-Arg-asn-Pra-Ile-X)-K-(FΦRRRR)-J]-BBM-resin (where X represents random positions). Screening of the focused library against K-Ras G12V did not identify any inhibitor of improved potency (Table 2, peptides **18**−**30**). The experiment did, however, provide some useful insights; e.g., a D-leucine, which should improve the proteolytic stability of the peptide, is tolerated at position 2 and an Asp, which improves the aqueous solubility, is accommodated at position 8 (Figure 1 and Table 2, peptide **20**). Alanine-scan analysis (replacement of each residue with Ala or D-Ala) revealed that Phg^3, Arg^4, and asn^5 are critical for binding to K-Ras, as substitution of any these residues reduced the K-Ras binding affinity by ≥3-fold (Table 2, peptides **31**−**34**). Thus, these residues were replaced with structurally similar amino acids to identify the most optimal side chain at each position. While most of the substitutions either had no effect or decreased the affinity, replacement of Phg^3 with Phe or Tyr resulted in modest increase in binding affinity (Table 2, K_{Dapp} of 0.80 and 0.66 μM for peptides **39** and **46**). In particular, replacement of Phg^3 in peptide **20** with Phe produced peptide **49** (Figure 1), which is the most potent K-Ras inhibitor of this series (K_{Dapp} = 0.21 μM). We also replaced the CPP motif ($F\Phi R_4$) with other Arg-rich sequences to test whether the CPP ring contributes to K-Ras binding. All of the substitutions resulted in either a loss or significant decrease of K-Ras binding affinity (Table 2, peptides **50**−**53**), strongly suggesting that the CPP ring participates in K-Ras binding. This is not surprising, as the effector-binding site of K-Ras is highly negatively charged[38] and many of the previously discovered cyclic peptide Ras inhibitors contained multiple arginine residues.[26−28] As a control, we also synthesized peptide **54**, which lacks the DCAI moiety but is otherwise identical to peptide **49** (Figure 1). Peptide **54** bound to K-Ras G12V with ~80-fold lower affinity than peptide **49** (K_{Dapp} = 17 μM; Figure S2).

Biochemical Characterization of Peptide 49. During the initial characterization of the hits and hit optimization, the binding experiments were performed with recombinant K-Ras G12V as purified from *Escherichia coli*. Because the recombinant protein contained a mixture of GTP- and GDP-bound forms (Ras-GTP and Ras-GDP, respectively), the values reported in Table 2 represent apparent dissociation constants (K_{Dapp}). To determine the actual K_D values and whether inhibitor **49** is selective for Ras-GTP, we prepared K-Ras G12V specifically loaded with GDP or GPPNP (a nonhydrolyzable GTP analog). Peptide **49** bound Ras-GDP and Ras-GPPNP with K_D values of 0.37 ± 0.09 and 0.86 ± 0.28 μM, respectively (Figure 2a). To test whether peptide **49** inhibits the Ras−Raf interaction, we first immobilized the biotinylated K-Ras G12V (which contained a mixture of GTP and GDP in the active site) onto streptavidin-coated agarose beads and incubated the beads with Texas red-labeled Ras-binding domain (RBD) of Raf (0.5 μM). Binding of Raf RBD to the immobilized K-Ras rendered the beads intensely fluorescent (Figure S3). In the presence of 8 μM peptide **49** (but not peptide **54**), however, binding of Raf RBD to the beads was largely abolished. We next employed a homogeneous time-resolved fluorescence (HTRF) assay to determine the potency of the inhibition. Briefly, biotinylated G12V K-Ras-GPPNP, glutathione-S-transferase (GST)-tagged Raf RBD, streptavidin-labeled with fluorescence acceptor d2, and anti-GST antibody labeled with fluorescence donor Tb were incubated with increasing concentrations of peptide **49** (unlabeled), and the time-resolved resonance energy transfer between the donor−acceptor pair was monitored. Peptide **49** inhibited the Ras-Raf interaction in a concentration-dependent manner, with a half maximal inhibitory concentration (IC_{50}) of 3.4 ± 0.7 μM (Figure 2b).

The ~80-fold difference in Ras binding affinity between peptides **49** and **54** suggests that the DCAI moiety of peptide

DOI: 10.1021/acscombsci.5b00164
ACS Comb. Sci. 2016, 18, 75−85

Table 2. Sequences and Binding Affinities of K-Ras Binding Peptides

	sequence[a]											
Pept		AA1	AA2	AA3	AA4	AA5	AA6	AA7	AA8	CPP motif		K_{Dapp} (μM)
2	*bicyclo* [Tm-			Arg	Asp	Phg	Pra*	asn		Lys	Phe-Nal-Arg-Arg-Arg-Arg	Dap]-Lys	NB
6				Phg	Arg	asn	Pra*	Ile					5.1 ± 2.5
12				Pra*	Ser	Phg	AcK	AcK					~ 20
13				Pra*	Arg	val	Asp	Ala					9.0 ± 4.7
14			Ala	Phg	Arg	asn	Pra*	Ile					6.4 ± 4.2
15				Phg	Arg	asn	Pra*	Ile	Ala				5.6 ± 1.0
16			Ala	Phg	Arg	asn	Pra*	Ile	Ala				1.8 ± 0.6
17		Ala	Ala	Phg	Arg	asn	Pra*	Ile	Ala				1.4 ± 0.5
18		ala	Abu	Phg	Arg	asn	Pra*	Ile	Abu				2.5 ± 0.7
19		Phg	Ile	Phg	Arg	asn	Pra*	Ile	Abu				2.4 ± 0.3
20		Ala	leu	Phg	Arg	asn	Pra*	Ile	Asp				1.1 ± 0.6
21		ala	Gln	Phg	Arg	asn	Pra*	Ile	Asp				2.0 ± 0.5
22		Ala	Orn	Phg	Arg	asn	Pra*	Ile	phe				6.3 ± 3.9
23		ala	Phg	Phg	Arg	asn	Pra*	Ile	phe				4.9 ± 1.4
25		ala	Abu	Phg	Arg	asn	Pra*	Ala	Abu				3.7 ± 0.7
26		Ala	leu	Phg	Arg	asn	Pra*	Asp					3.4 ± 0.6
27		Ala	leu	Phg	Arg	asn	Pra*	Ala	Asp				7.7 ± 2.8
28		ala	Abu	Phg	Arg	asn	Pra*	Ile	Nle				ND
29		ala	Ala	Phg	Arg	asn	Pra*	Ile	asn				ND
30		Arg	Nle	Phg	Arg	asn	Pra*	Ile	Ser				4.0 ± 0.7
31		Ala	Ala	Phg	Arg	asn	Pra*	Ala					2.2 ± 0.2
32		Ala	Ala	Phg	Arg	Ala	Pra*	Ala					7.1 ± 1.2
33		Ala	Ala	Phg	Ala	asn	Pra*	Ala					15 ± 2
34		Ala	Ala	Ala	Arg	asn	Pra*	Ala					4.2 ± 1.7
35		Ala	leu	Phg	Arg	asn	Pra*	Val	Asp				2.1 ± 0.5
36		Ala	Ala	Phg	Arg	asn	Pra*	Val	Ala				ND
37		Ala	Ala	Phg	Arg	asn	Pra*	Leu	Ala				3.7 ± 0.9
38		Ala	Ala	Phg	Arg	asn	Pra*	Nle	Ala				4.1 ± 1.7
39		Ala	Ala	Phe	Arg	asn	Pra*	Ile	Ala				0.80 ± 0.11
40		Ala	Ala	Phg	Arg	gln	Pra*	Ile	Ala				4.8 ± 0.5
41		Ala	Ala	Phg	Arg	asn	Pra*	Thr	Ala				4.2 ± 1.8
42		Ala	Ala	Phg	Arg	asn	Pra*	Phe	Ala				> 10
43		Ala	Ala	Phg	Arg	ser	Pra*	Ile	Ala				2.7 ± 1.4
44		Ala	Ala	Phg	Arg	asp	Pra*	Ile	Ala				> 10
45		Ala	Ala	Fpa	Arg	asn	Pra*	Ile	Ala				1.9 ± 0.9
46		Ala	Ala	Tyr	Arg	asn	Pra*	Ile	Ala				0.66 ± 0.47
47		Ala	Ala	Trp	Arg	asn	Pra*	Ile	Ala				ND
48		Ala	Ala	homoF	Arg	asn	Pra*	Ile	Ala				> 10
49		Ala	leu	Phe	Arg	asn	Pra*	Ile	Asp				0.21 ± 0.10
50		Ala	leu	Phe	Arg	asn	Pra*	Ile	Asp		Nal-Phe-Arg-Arg-Arg-Arg		0.33 ± 0.23
51		Ala	leu	Phe	Arg	asn	Pra*	Ile	Asp		Arg-Arg-Phe-Arg-Nal-Arg		0.31 ± 0.11
52		Ala	leu	Phg	Arg	asn	Pra*	Ile	Asp		phe-Nal-Arg-arg-Arg-arg		> 10
53		Ala	Ala	Phe	Arg	asn	Pra*	Ile	Ala				> 10
54		Ala	leu	Phe	Arg	asn	Pra	Ile	Asp		Phe-Nal-Arg-Arg-Arg-Arg		17 ± 11

[a]Abbreviations: Abu, L-2-aminobutyric acid; ala, D-alanine; arg, D-arginine; asn, D-asparagine; asp, D-aspartic acid; Dap, L-2,3-diaminopropanoic acid; Fpa, L-4-fluorophenylalanine; homoF, L-homophenylalanine; leu, D-leucine; Nal, L-naphthylalanine; Nle, norleucine; Orn, L-ornithine; phe, D-phenylalanine; Phg, L-phenylglycine; Pra, L-propargylglycine; Pra*, DCAI-modified propargylglycine; ser, D-serine; Tm, trimesic acid.

49 engages in critical interactions with the Ras protein surface, presumably by inserting into the same DCAI-binding pocket as previously observed by X-ray crystallography.[19] To test this possibility, we performed an FA-based competition assay in which binding of FITC-labeled peptides **49** and **54** to K-Ras G12V was examined in the presence of increasing concentrations of DCAI (Figure S4). As expected, DCAI concentration-dependently inhibited the binding of peptide **49** to K-Ras, with an IC_{50} value (0.84 ± 0.22 mM) similar to the K_D value (1.1 mM) previously reported for DCAI binding to K-Ras.[19] In contrast, DCAI did not affect the binding of peptide **54** to K-Ras until at 2.5 mM, the highest concentration tested. These results, together with the observation that peptide **49** inhibits the Ras-Raf interaction, strongly suggest that peptide **49** binds K-Ras at or near the effector-binding site with its DCAI moiety reaching into the canonical DCAI-binding pocket. Alternatively, binding by DCAI may induce a conformational change in the K-Ras structure and allosterically inhibit the binding of peptide **49** at a different site. However, such a conformational change would be expected to similarly affect the binding of peptide **54**, which was not the case.

DOI: 10.1021/acscombsci.5b00164
ACS Comb. Sci. 2016, 18, 75−85

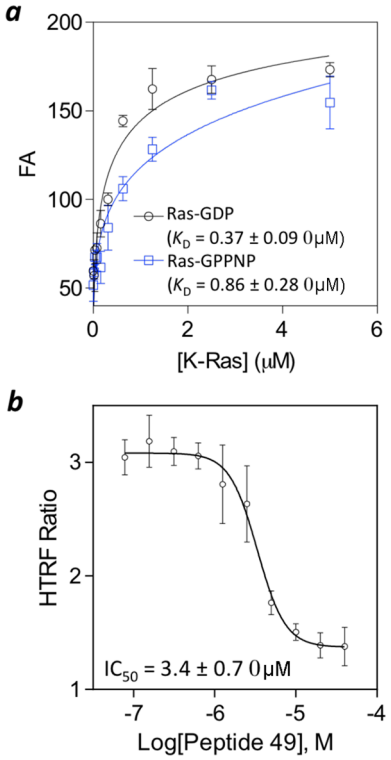

Figure 2. (a) Binding of FITC-labeled peptide **49** to G12V K-Ras-GDP and K-Ras-GPPNP as monitored by FA. (b) Inhibition of K-Ras-GPPNP-Raf RBD interaction by unlabeled peptides **49** as analyzed by the HTRF assay. Data reported represent the mean ± SD of three independent experiments.

Finally, to assess the specificity of peptide **49** for K-Ras, we tested it for binding to several arbitrarily selected proteins including bovine serum albumin (BSA), GST-NEMO, protein tyrosine phosphatase 1B, and peptidyl-prolyl isomerase Pin1 by FA analysis. Peptide **49** showed moderate binding to BSA (K_D = 5.1 ± 1.2 μM) but no binding to any of the other proteins (Figure S5). We therefore conclude that peptide **49** is a selective ligand for K-Ras and an orthosteric inhibitor of the Ras-Raf interaction.

Biological Activity. The antiproliferative activity of peptides **49** and **54** were tested against H441 human lung cancer cells, which harbor a K-Ras G12V mutation, by using the MTT cell viability assay.[39] Peptide **49** reduced the cell viability in a dose-dependent manner, with an LD_{50} value of ∼17 μM (Figure S6). As expected, peptide **54** was less active under the same conditions, causing significant reduction in cell viability only at the highest inhibitor concentration tested (40 μM). Peptide **49** was also active against a panel of other human lung and pancreatic cancer cell lines, among which the H1299 lung cancer cell line was most sensitive to the bicyclic Ras inhibitor (LD_{50} ∼ 8 μM; Figure 3a). Again, peptide **54** was less active, having an LD_{50} > 40 μM. H1299 cells express a Q61K N-Ras mutant and were previously found to be most sensitive to another Ras inhibitor, cyclorasin 9A5, among a panel of lung and pancreatic cancer cell lines tested.[28] We thus chose the H1299 cell line for further mechanistic investigation.

Since K-Ras is an intracellular protein, we assessed the membrane permeability of peptides **49** and **54** by two different methods. First, H1299 cells were treated with 5 μM FITC-labeled peptide **49** or **54** and examined by live-cell confocal microscopy. Peptide **49** was efficiently internalized by the cancer cells (Figure 3b). Although the internalized peptide

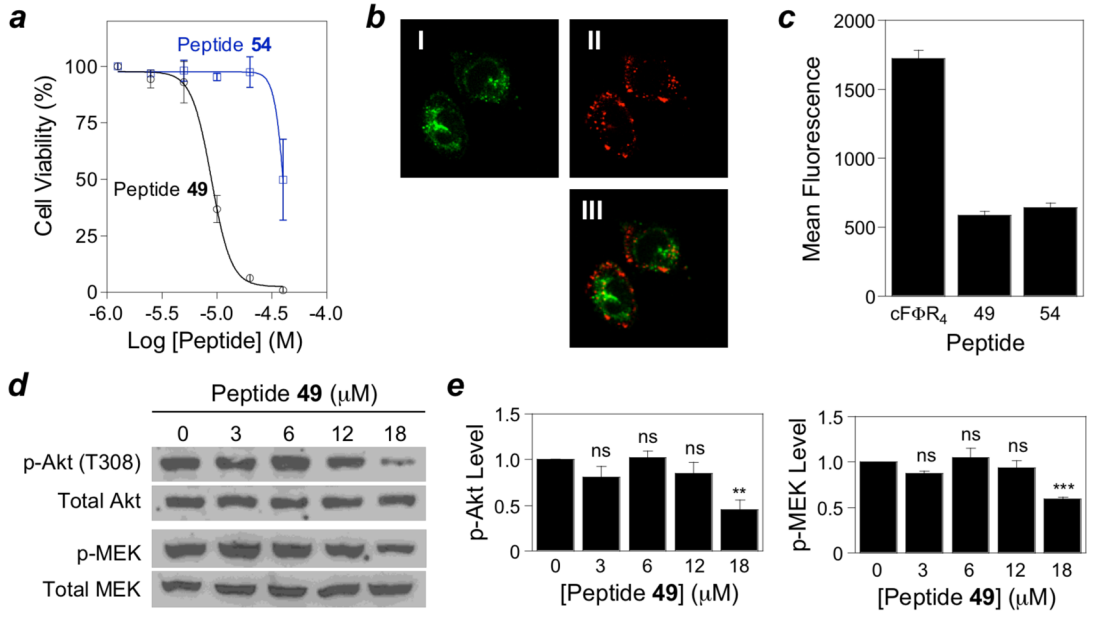

Figure 3. Inhibition of Ras signaling in human lung cancer H1299 cells by peptide **49**. (a) MTT assay of cell viability as a function of Ras inhibitor concentration. (b) Live-cell confocal microscopic images (same Z-section) of lung cancer cells after treatment for 2 h with 5 μM FITC-labeled peptide **49** (I) or endocytosis marker dextran^{Rho} (1.0 mg/mL, II) and the merge of I and II (III). (c) Flow cytometry analysis of the mean fluorescence intensity of cells after treatment with 5 μM FITC-labeled cFΦR_4, peptide **49**, or peptide **54** for 2 h. (d) Western blots showing the dose-dependent inhibition of MEK and Akt phosphorylation in H1299 cells by peptide **49**. The cells were treated with peptide **49** for 12 h and stimulated with 50 ng/mL epidermal growth factor for 10 min prior to lysis. (e) Quantitation of Western blot results from d and the data reported are relative to that of untreated cells and represent the mean ± SD from three independent experiments. ns, not significant; **, p < 0.01; ***, p < 0.001.

DOI: 10.1021/acscombsci.5b00164
ACS Comb. Sci. 2016, 18, 75−85

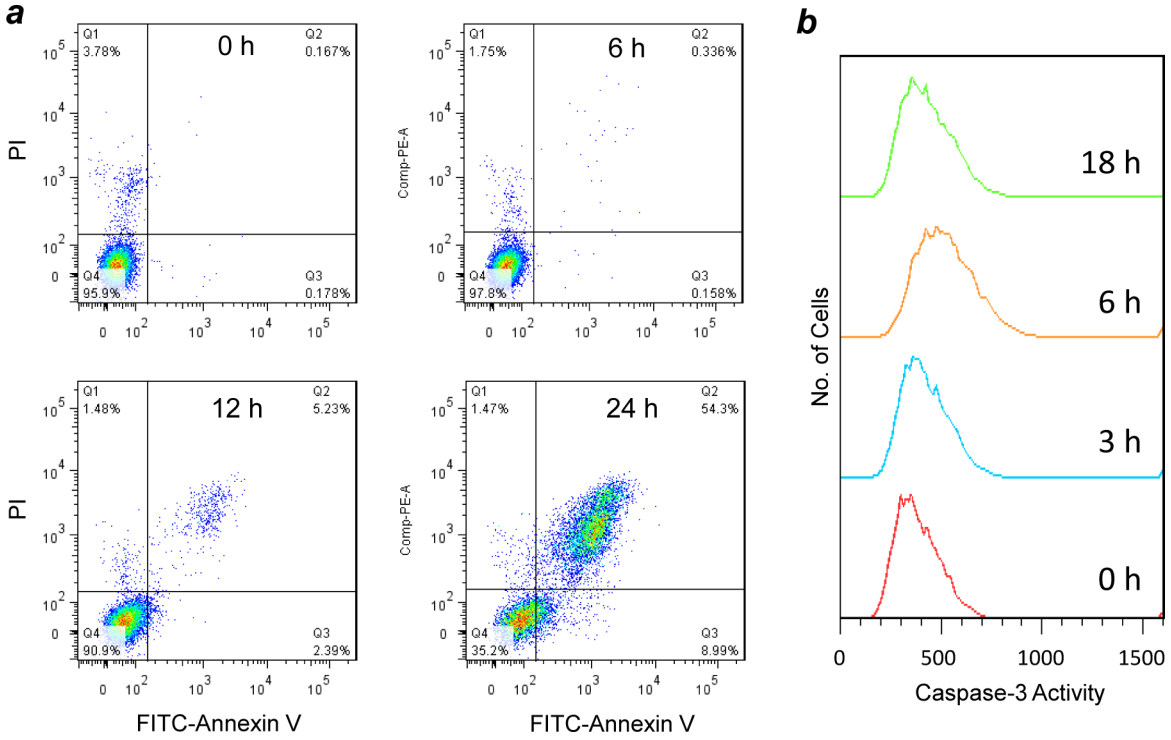

Figure 4. Induction of apoptosis of H1299 cells by peptide **49**. (a) Flow cytometry analysis of H1299 cells after treatment with 10 μM peptide **49** for varying periods of time (0−24 h) and stained with FITC-annexin V and propidium iodide (PI). The percentage of cells in each quartile is indicated. (b) Activation of caspase-3 activity in H1299 cells by peptide **49** (20 μM) as monitored by anticaspase-3 immunostaining and flow cytometry.

produced punctate fluorescence patterns, its intracellular distribution did not overlap with that of rhodamine-labeled dextran (an endocytosis marker), suggesting that the peptide had escaped from the endosome into the cytosol. The punctate fluorescence pattern is likely due to binding of peptide **49** to K-Ras and other Ras isoforms (i.e., H- and N-Ras), which are localized on the plasma membrane as well as endomembranes including the Golgi and recycling endosomes.[40] Peptide **54** showed a largely similar intracellular distribution. Second, H1299 cells after treatment for 2 h with 5 μM FITC-labeled peptide **49** or **54** were analyzed by flow cytometry to quantify the total amounts of the internalized peptides and compared with those of cFΦR$_4$ (Figure 3c). Peptides **49** and **54** entered the cancer cells with similar efficiencies, which were ∼3-fold lower than that of cFΦR$_4$, one of the most active CPPs reported so far.[5−7]

Among the signaling cascades downstream of Ras, the Raf/MEK/ERK and PI3K/PDK1/Akt pathways are well characterized.[6] The former controls cell proliferation, while the latter regulates cell survival and differentiation. Stimulation of cells with an extracellular signal (e.g., a growth factor) causes the exchange of Ras-bound GDP into GTP, and the resulting active Ras binds Raf and PI3K, leading to the phosphorylation and activation of MEK, ERK, and Akt kinases. We therefore examined the effect of peptide **49** on the phosphorylation of MEK and Akt, by immunoblotting with antibodies specific for phosphorylated MEK (p-MEK) and Akt (p-Akt at Thr308, which is phosphorylated by PDK1[41]). As expected, treatment of H1299 cells with peptide **49** resulted in dose-dependent reduction of epidermal growth factor (EGF)-induced p-MEK (up to 50%) and p-Akt levels (up to 60%), while the total cellular concentrations of MEK and Akt were not affected (Figure 3d and e). Peptide **54** showed no effect under similar conditions. Inhibition of MEK and Akt phosphorylation by peptide **49** was also observed in H441 cells, although the effects were less dramatic (Figure S6).

Dual inhibition of MEK and PI3K signaling by kinase inhibitors had previously been shown to cause synergistic reduction in cell proliferation and an increase in apoptotic cell death of Ras mutant cancer cells.[42,43] Cyclorasin 9A5, which orthosterically blocks both Ras-Raf and Ras-PI3K interactions, also caused apoptosis of H1299 and other cancer cells.[28] We therefore tested the ability of peptide **49** to induce apoptosis of Ras mutant cancer cells. H1299 cells were treated with 10 μM peptide **49** and stained with FITC-labeled annexin V and propidium iodide, which detect apoptotic and dead cells, respectively. There was little cell death within the first 6 h; however, cell death started to occur at 12 h (∼5% cells) and reached 54% after 24 h (Figure 4a). At 12 and 24 h, a fraction of the cell population showed increased staining by annexin V but not propidium iodide, a hallmark of cells undergoing apoptosis. Consistent with apoptotic cell death, the activity of caspase-3, a cysteine protease that plays a central role in apoptosis, increased by 1.3-fold at 6 h and subsequently declined (Figure 4b).

DISCUSSION

The primary motivation for this work is to test the generality of the bicyclic delivery method[8] for transporting peptide cargos into the cytosol of mammalian cells. In this study, four peptides selected from a combinatorial library of 5.7 × 10^6 sequences on the basis of K-Ras binding (hits **2**, **6**, **12**, and **13**) and two peptides derived from hit optimization (peptides **49** and **54**) were tested for cellular uptake. Although no further attempt was made to improve their cellular uptake efficiency, all six peptides were readily cell permeable. We previously examined

DOI: 10.1021/acscombsci.5b00164
ACS Comb. Sci. 2016, 18, 75−85

over a dozen other bicyclic peptides containing FΦR$_4$ or R$_4$ΦF in one ring and diverse sequences including negatively charged phosphates and phosphonates in the second ring.[7−9] Again, all of the bicyclic peptides tested were cell permeable. On the basis of these data, we conclude that the bicyclic system provides a general approach to delivering peptide cargos into mammalian cells and that most (if not all) members of the bicyclic peptide library are cell permeable. To the best of our knowledge, this is the first example of a cell-permeable peptide library. A key consideration during the library design was the choice of trimesoyl group as a rigid and planar scaffold, which presumably orients the CPP and cargo moieties away from each other, minimizing any mutual interference.[8,31] Of course, it is also possible for a cargo motif (e.g., peptides containing Arg and Phe/Trp residues) to contribute positively to membrane binding and enhance cellular entry. Similarly, the CPP motif may interact with the target protein and increase the potency and/or specificity of the ligand. The latter is clearly the case for peptide **49**.

To demonstrate the utility of the cell-permeable peptide library, we selected the oncogenic G12V K-Ras, a notoriously difficult drug target, to provide a rigorous test of our methodology. Screening of the bicyclic peptide library indeed resulted in peptides **6**, **12**, and **13** as moderately potent, cell-permeable K-Ras inhibitors. Subsequent optimization of hit peptide **6** through medicinal chemistry afforded peptide **49** as a relatively potent direct Ras inhibitor. Its ability to disrupt the Ras-Raf interaction and compete with DCAI for binding to K-Ras suggests that it binds to a similar site to cyclorasin 9A5,[28] which extends from the DCAI-binding pocket[19] to the effector-binding site. Mapping the precise binding site of inhibitor **49** will require structural studies in the future. Since the effector-binding site is conserved among all Ras isoforms and distant from the activating mutations (e.g., G12, G13, and Q61), peptide **49** is expected to inhibit all Ras isoforms, either wild-type or mutant. Peptide **49** inhibits Ras signaling in cancer cells and induces apoptotic cell death of the cancer cells, although relatively high inhibitor concentrations are required. The relatively weak cellular activity is likely caused by a combination of two factors. First, peptide **49** has only moderate binding affinity to Ras-GTP (K_D = 0.86 μM), the active form of Ras. Second and more importantly, peptide **49** binds more tightly to the inactive Ras-GDP form (K_D = 0.37 μM). Since cells contain higher concentrations of Ras-GDP (0.4−20 μM) than Ras-GTP (0−50 nM),[44] the internalized peptide **49** is most likely sequestered by Ras-GDP and rendered "inactive." In retrospect, we would have benefited from employing Ras-GPPNP during library screening and hit optimization instead of the recombinant K-Ras G12V as purified from *E. coli* (which contained predominantly Ras-GDP). Nonetheless, the current work demonstrates that it is now feasible to obtain biologically active cyclic peptidyl ligands against an intracellular protein by screening a combinatorial library.

In conclusion, we have developed a general strategy for synthesizing and screening combinatorial libraries of cell-permeable bicyclic peptides against intracellular PPIs. Application of this strategy to K-Ras, a prototypical "undruggable" target, resulted in a relatively potent, selective inhibitor that induces apoptotic death of cancer cells. The Ras inhibitor may be further improved to provide useful tools for investigating the biological function of Ras and potential anticancer therapeutics. The library method should be readily applicable to other intracellular protein targets.

EXPERIMENTAL SECTION

Materials. Reagents for peptide synthesis and other materials are described in the Supporting Information. All of the peptides used in this work were purified by reversed-phase HPLC to at least 95% homogeneity, and their authenticity was confirmed by MALDI-TOF mass spectrometry.

Preparation of Ras-GDP and Ras-GPPNP. Expression and purification of recombinant K-Ras G12V in *E. coli* and nucleotide exchange into GDP or guanosine 5′-[β,γ-imido]-triphosphate (GPPNP) were carried out as previously described.[19] The nucleotide loading was assessed by reversed-phase HPLC under ion pairing conditions as previously described.[45]

Synthesis of 4,6-Dichloro-2-methyl-3-azidoethylindole (DCAI-N$_3$). DCAI (200 mg, 0.82 mmol), $CuSO_4 \cdot 5H_2O$ (2 mg, 0.0082 mmol), and K_2CO_3 (295 mg, 2.14 mmol) were stirred in 5 mL of methanol at room temperature. Imidazole-1-sulfonyl azide hydrochloride[46] (341 mg, 1.64 mmol) was added, and the mixture was stirred for 14 h at room temperature. After evaporation of the solvent in vacuo, 10 mL of water was added, and the mixture was acidified to pH 3 with the addition of 6 M HCl. The mixture was extracted with ethyl acetate (3 × 15 mL) and the combined organic phase was dried with $MgSO_4$ and evaporated to afford DCAI-N$_3$ as a brown solid. ^{1}H NMR (400 MHz, $CDCl_3$): δ 7.93 (s, br, 1H), 7.17 (d, 1H), 7.07 (d, 1H), 3.52 (t, 2H), 3.17 (t, 2H), 2.41 (s, 3H). ^{13}C NMR (100 MHz, $CDCl_3$): δ 136.8, 134.8, 126.8, 125.5, 123.9, 121.0, 109.4, 108.5, 53.1, 24.9, 11.7. HRMS (ESI+) Calculated for $C_{11}H_{11}Cl_2N_4$ (M + H$^+$): 271.0512. Found: 271.0764.

Library Synthesis. Peptide library I was synthesized on 2.0 g of TentaGel S NH$_2$ resin (90 μm; Scheme S1). All of the manipulations were performed at room temperature unless otherwise noted. The linker sequence (BBM) was synthesized using 4 equiv of Fmoc amino acid, 4 equiv of HATU, and 8 equiv of *N*-methylmorpholine (NMM). The coupling reaction was allowed to proceed for 2 h, and the beads were washed with DMF (3 × 10 mL) and dichloromethane (DCM, 3 × 10 mL). The Fmoc group was removed with 20% piperidine in DMF (2 × 10 min), and the beads were exhaustively washed with DMF (6 × 10 mL). After the synthesis of linker, the resin was washed with DCM (2 × 10 mL) and DMF (2 × 10 mL) and was soaked in DMF for 15 min, followed by mixtures of 3:1 DMF/water, 1:1 DMF/water, 1:3 DMF/water, and finally in 100% degassed water overnight at room temperature. The water was drained, and the resin was quickly suspended in a solution of Fmoc-*N*-hydroxysuccinimide ester (Fmoc-OSu; 0.21 mmol, 0.4 equiv) in 15 mL of 1:1 (v/v) DCM/diethyl ether. The mixture was incubated on a rotary shaker for 30 min at room temperature. The beads were washed with 1:1 DCM/diethyl ether (3 × 10 mL) and DMF (5 × 10 mL) to remove water from the beads and then treated with 10 equiv of di-*tert*-butyl dicarbonate and 0.05 equiv of 4-dimethylaminopyridine in DMF (40 min). After washing with DMF, the Fmoc group on the surface peptides was removed, and the resin was treated with 4 equiv of Fmoc-Dap(Alloc)-OH, 4 equiv of HATU, and 8 equiv of NMM. The Boc group was removed by treating the resin with trifluoroacetic acid (TFA)/H$_2$O (95:5) for 2 h. The resin was treated with 20% piperidine in DMF (2 × 10 min) to remove the Fmoc group and split into two equal portions. The CPP sequence Phe-Nal-(Arg)$_4$ was coupled to the first portion, whereas (Arg)$_4$-Nal-Phe was added to the second portion, by using standard Fmoc/HATU chemistry. The resin was

DOI: 10.1021/acscombsci.5b00164
ACS Comb. Sci. 2016, 18, 75−85

combined, treated with 20% piperidine in DMF (2 × 10 min), and treated with 4 equiv of Fmoc-Lys(Mtt)-OH, 4 equiv of HATU, and 8 equiv of NMM. Next, the five random residues were added by the split-and-pool synthesis method. At each random position, the resin was split into two unequal portions (20% and 80% by weight). The smaller portion (20%) was coupled with 3.6 equiv of Fmoc-Lys(Ac)-OH plus 0.4 equiv of Fmoc-Pra-OH, 4 equiv of HATU, and 8 equiv of NMM. The larger portion (80%) was further split into 25 equal portions, and each portion was reacted with a different Fmoc-amino acid. To complete the synthesis of library I, the split-and-pool procedure was repeated four times.

Prior to cyclization, the Mtt group on the Lys side chain was removed with 2% TFA and 2.5% triisopropylsilane (TIPS) in DCM (10 × 3 min) and replaced with an Fmoc group by treating the resin with 10 equiv of Fmoc-OSu and 5 equiv of NMM for 20 min. The Alloc group on the Dap side chain was removed by treating the resin with 0.5 equiv of $Pd(PPh_3)_4$ and 10 equiv of phenylsilane ($PhSiH_3$) in DCM (3 times with 15 min and fresh reagents each time). The resin was washed with DCM (5 times), DMF (5 times), and 1% sodium dimethyldithiocarbamate (SDDC) in DMF. The resin was incubated with 1% SDDC in DMF for 10 min and washed with DMF (10 times). The resin (~100 mg each time) was transferred to a 4 mL glass vial, and 300 μL of DMF and 30 μL of *tert*-butyl alcohol were added. In a microcentrifuge tube, 30 μL of 500 mM aqueous ascorbic acid was quickly mixed with 30 μL of 500 mM aqueous cupric sulfate. A total of 30 μL of the resulting solution and 30 μL of the DCAI-N_3 solution (50% w/v in DMF) were added to the resin (the final concentration of DCAI-N_3 in the reaction mixture was 0.15 M). The reaction mixture was incubated overnight at room temperature on a rotary shaker. The resin was transferred to a 1 mL Bio-Rad column and washed with DMF (5 × 1 mL) and 1% SDDC in DMF (5 × 1 mL) and incubated with 1% SDDC in DMF (1 mL) for 15 min. After washing with DMF (5 × 1 mL), the resin was reacted with trimesic acid (22 mg, 0.104 mmol), HATU (35 mg, 0.091 mmol), and NMM (23 μL, 0.208 mmol) for 1 h. The resin was washed with DMF (5 × 1 mL) and treated with 2% 1,8-diazabicycloundec-7-ene (DBU) in DMF (1 mL for 10 min) to remove the Fmoc groups. The resin was washed with DMF (5 × 1 mL) and 1 M hydroxybenzotriazole (HOBt) in DMF (2 × 1 mL) and incubated in 1 M HOBt in DMF for 15 min. After washing with DMF (5 × 1 mL), the resin was treated with PyBOP (68 mg, 0.13 mmol), HOBt (20 mg, 0.13 mmol), and NMM (29 μL, 0.26 mmol) for 90 min to cyclize the surface peptides. The resin was washed with DMF (5 × 1 mL) and DCM (5 × 1 mL), and side chain deprotection was carried out by treatment with a modified reagent K (7.5% phenol, 5% water, 5% thioanisole, 2.5% ethanedithiol, 2.5% TIPS, 1.25% anisole in TFA) for 2.5 h. The resin was washed exhaustively with DCM, dried, and stored at −20 °C until use.

Library Screening. The resin-bound peptide library (100 mg) was washed with DMF (5 × 1 mL), water (5 × 1 mL), and PBS (5 × 1 mL). The resin was incubated with a blocking buffer [PBS plus 3% bovine serum albumin (BSA)] for 1 h at 4 °C. The resin was incubated with 100 nM biotinylated GST-K-Ras in 1 mL of the blocking buffer overnight at 4 °C. The resin was washed twice with the blocking buffer (1 mL), resuspended in 1 mL of the blocking buffer containing 1 μg/mL streptavidin-alkaline phosphatase conjugate (SA-AP, Promega), and incubated for 10 min at 4 °C with gentle mixing. The resin was drained and washed with the blocking buffer (2 × 1 mL) and SA-AP reaction buffer (30 mM Tris HCl, pH 8.5, 100 mM NaCl, 5 mM $MgCl_2$, 20 μM $ZnCl_2$, and 0.05% Tween 20; 2 × 1 mL). The resin was transferred to a Petri dish by using 1.8 mL of the SA-AP reaction buffer (3 × 600 μL). A 5 mg/mL solution of 5-bromo-4-chloro-3-indolyl phosphate (BCIP, Sigma-Aldrich; 200 μL) was added to the dish, and the mixture was incubated on a rotary shaker. Turquoise color developed on positive beads in ~30 min, when the staining reaction was terminated by the addition of 500 μL of 1 M HCl. The positive beads were isolated manually with a micropipet under a dissecting microscope and individually sequenced by the PED-MS method as previously described.[37]

Synthesis and Labeling of Individual Peptides. Individual peptides were each synthesized on 100 mg of Rink amide resin. The synthesis began by attaching Fmoc-Lys(Boc)-OH to the resin to provide a handle for dye labeling. Synthesis of other positions was carried out using standard Fmoc/HATU chemistry. Click chemistry and cyclization of the individual peptides were carried out in the same manner as described for the library synthesis. Cleavage and deprotection of resin-bound peptides were carried out using the modified reagent K at room temperature for 2.5 h. After evaporation of solvents, the mixture was triturated three times with 20 volumes of cold ethyl ether. The precipitate was collected and dried under a vacuum. The crude peptides were purified by reversed-phase HPLC equipped with a semipreparative C_{18} column. The identity of each peptide was confirmed by MALDI-TOF mass spectrometric analysis. The solvent was removed, and the purified peptide (~1 mg) was dissolved in 15 μL of DMSO, 15 μL of DMF, and 15 μL of 100 mM $NaHCO_3$ (pH 8.5). The labeling reaction was initiated by the addition of 0.1 mg of FITC dissolved in 10 μL of DMSO and allowed to proceed for 30 min in the dark. The reaction was quenched by the addition of 5 μL of 50% TFA in water. The labeled peptide was purified again by reversed-phase HPLC. The identity of each peptide was confirmed by MALDI-TOF mass spectrometric analysis.

Fluorescence Anisotropy. For FA experiments, K-Ras protein (non-GST fusion, 0−20 μM) was incubated with FITC-labeled peptide (100 nM) in 20 μL of PBS for 2 h at room temperature. The FA values were measured on a Molecular Devices Spectramax M5 spectrofluorimeter, with excitation and emission wavelengths at 470 and 530 nm, respectively. Equilibrium dissociation constants (K_D) were determined by plotting the FA values as a function of K-Ras concentration and fitting the data to the equation

$$Y = \frac{\left(A_{\min} + \left(A_{\max} \times \frac{Q_b}{Q_f} - A_{\min}\right)\left(\frac{(L + x + K_d) - \sqrt{((L + x + K_d)^2 - 4Lx)}}{2L}\right)\right)}{\left(1 + \left(\frac{Q_b}{Q_f} - 1\right)\left(\frac{(L + x + K_d) - \sqrt{((L + x + K_d)^2 - 4Lx)}}{2L}\right)\right)}$$

where Y is the measured anisotropy at a given K-Ras concentration x, L is the peptide concentration, Q_b/Q_f is the correction factor for dye−protein interaction, A_{max} is the maximum anisotropy at saturating K-Ras concentration, and A_{min} is the minimum anisotropy.

HTRF Assay. Recombinant biotinylated G12V K-Ras-GPPNP (no GST, 50 nM), GST-RBD (50 nM), streptavidin-labeled with acceptor d2 (2 μg/mL), anti-GST monoclonal antibody labeled with donor Tb (0.25 μg/mL), and varying concentrations of cyclic peptide (0−40 μM) were mixed in PBS (total volume of 20 μL) in a 384-well plate. The plate was

DOI: 10.1021/acscombsci.5b00164
ACS Comb. Sci. 2016, 18, 75−85

incubated 2 h at room temperature, and the HTRF signals were measured on a Molecular Devices Spectramax M5 plate reader and plotted as a function of the cyclic peptide concentration. The data were analyzed using Prism 6.0 from Graphpad Software, Inc. (La Jolla, CA), and IC_{50} values were obtained by fitting the data to the dose−response inhibition curves.

Cell Culture. H441 and H1299 cells were maintained in a growth medium consisting of RPMI, 10% fetal bovine serum (FBS), and 1% penicillin/streptomycin. Cells were cultured in a humidified incubator at 37 °C with 5% CO_2.

MTT Assay. A total of 100 μL of H441 or H1299 cells (0.5×10^5 cells/mL) were placed in each well of a 96-well culture plate and allowed to grow overnight. Varying concentrations of peptide inhibitor (0−40 μM) were added to the wells, and the cells were incubated at 37 °C with 5% CO_2 for 24 h. A total of 10 μL of a MTT stock solution (5 mg/mL) was added into each well. The plate was incubated at 37 °C for 4 h. Then, 100 μL of SDS-HCl solubilizing buffer was added into each well, and the resulting solution was mixed thoroughly. The plate was incubated at 37 °C overnight. The absorbance of the formazan product was measured at 570 nm using a Molecular Devices Spectramax M5 plate reader. The cells without any peptide added were treated as control.

Confocal Microscopy. A total of 1 mL of H1299 cell suspension (~1.5×10^4 cells) was seeded in a 35 mm glass-bottomed microwell dish (MatTek) and cultured overnight. Cells were gently washed with PBS twice and treated with FITC-labeled peptide (5 μM) in phenol-red free and HEPES supplemented RPMI containing 10% FBS at 37 °C for 2 h in the presence of 5% CO_2. After removal of the medium, the cells were gently washed with DPBS twice and imaged on a Visitech Infinity 3 Hawk 2D-array live cell imaging confocal microscope equipped with 60× oil objective. Data were analyzed using MetaMorph Premier (Molecular Devices).

Immunoblot Analysis. H1299 cells were grown in a 6-well plate to 80% confluency. The cells were treated with 0, 3, 6, 12, or 18 μM peptide **49** for 12 h followed by stimulation with EGF (50 ng/mL) for 10 min. The cells were washed with cold PBS and lysed in 100 μL of lysis buffer containing protease and phosphatase inhibitors for 30 min on ice and scraped off the plate. Each sample was combined with 100 μL of SDS-PAGE loading buffer and boiled for 5 min. The mixture was centrifuged at 13 000 rpm for 10 min, and the supernatant was separated by SDS-PAGE. The proteins were transferred to a nitrocellulose membrane and probed with the following antibodies: p-MEK1/2 (9121S), p-Akt(Thr308) (9275S), MEK1/2 (9122S), and Akt (9272S). The primary antibodies were detected using Clean-Blot IP detection reagent. The immunoblots were visualized using Supersignal West Femto maximum sensitivity substrate from Thermo. Experiments with H441 cells were carried out similarly, except that the cells were treated with 0, 5, 10, 20, and 40 μM peptide **49** for 5 h followed by stimulation with EGF (50 ng/mL) for 10 min.

Flow Cytometry. H1299 cells were seeded in 12-well plates and allowed to grow overnight in Advanced RPMI medium supplemented with 10% FBS and 1% penicillin-streptomycin. The cells were treated with 20 μM of peptide **49** for 6 h. The cells were trypsinized and washed with cold PBS twice. The cells were treated with BD Cytofix/Cytoperm solution (BD biosciences) for 30 min on ice. The cells were pelleted, washed with BD Perm/Wash buffer (BD biosciences) twice, and incubated with 20 μL of FITC-labeled anti-Active Caspase-3 antibody in 100 μL of BD Perm/Wash buffer for 30 min at room temperature. The cells were washed with 1 mL of BD Perm/Wash buffer and resuspended in 0.5 mL of BD Perm/Wash buffer and analyzed by FACS.

For propidium iodide and Annexin V staining, H1299 cells were seeded in six-well plates and cultured with RPMI-1640 media supplemented with 10% FBS. On the day of the experiment, cells were incubated with varying concentrations of peptide **49** for varying lengths of time. After the incubation, the media containing floating cells were collected into individual 15-mL centrifuge tubes. The adherent cells were trypsinized for 5 min and combined with their corresponding floating cell fractions. The combined cells were washed twice with DPBS and an Annexin assay binding buffer. A total of 100 μL of staining solution (containing 5 μL of Annexin-FITC and 5 μL of PI solution) was added, and the cells were gently mixed by vortexing. After 15 min of incubation at room temperature in the dark, 400 μL of the binding buffer was added, and the resulting cell suspension was analyzed by FACS.

To analyze the cellular uptake of peptides, H1299 cells were cultured in 12-well plates (1.5×10^5 cells per well) for 24 h. On the day of the experiment, the cells were incubated for the 2 h with 5 μM FITC-labeled peptide in phenol-red free and HEPES supplemented RPMI containing 10% FBS at 37 °C in the presence of 5% CO_2. At the end of incubation, the cells were washed with PBS twice, detached from the plate with 0.25% trypsin, diluted into clear RPMI, pelleted at 250*g* for 5 min, washed twice with PBS and resuspended in PBS containing 1% bovine serum albumin, and analyzed on a BD FACS LSR II flow cytometer. Flow cytometry data were analyzed using the Flowjo (Tree Star).

■ ASSOCIATED CONTENT

Supporting Information

The Supporting Information is available free of charge on the ACS Publications website at DOI: 10.1021/acscombsci.5b00164.

Experimental details and additional data (PDF)

■ AUTHOR INFORMATION

Corresponding Author

*Tel.: 614-688-4068. Fax: 614-292-1685. E-mail: pei.3@osu.edu.

Author Contributions

†These authors contributed equally.

Notes

The authors declare no competing financial interest.

■ ACKNOWLEDGMENTS

This work was supported by the National Institutes of Health (GM062820 and GM110208).

■ ABBREVIATIONS:

β-Ala, 3-aminopropanoic acid; Abu, L-2-aminobutyric acid; ala, D-alanine; arg, D-arginine; asn, D-asparagine; asp, D-aspartic acid; CPP, cell-penetrating peptide; Dap, L-2,3-diaminopropanoic acid; DCAI, 4,6-dichloro-2-methyl-3-aminoethylindole; Fpa, L-4-fluorophenylalanine; homoF, L-homophenylalanine; leu, D-leucine; Nal, L-naphthylalanine; Nle, norleucine; Orn, L-ornithine; phe, D-phenylalanine; Phg, L-phenylglycine; Pra, L-propargylglycine; Pra*, DCAI-modified propargylglycine; RBD, Ras-binding domain; ser, D-serine; Tm, trimesic acid

DOI: 10.1021/acscombsci.5b00164
ACS Comb. Sci. 2016, 18, 75−85

REFERENCES

(1) Verdine, G. L.; Walensky, L. D. The challenge of drugging undruggable targets in cancer: Lessons learned from targeting BCL-2 family members. *Clin. Cancer Res.* **2007**, *13*, 7264−7270.

(2) Wells, J.; McClendon, C. Reaching for high-hanging fruit in drug discovery at protein−protein interfaces. *Nature* **2007**, *450*, 1001−1009.

(3) Nevola, L.; Giralt, E. Modulating protein−protein interactions: the potential of peptides. *Chem. Commun.* **2015**, *51*, 3302−3315.

(4) Walensky, L. D.; Bird, G. H. Hydrocarbon-stapled peptides: principles, practice, and progress. *J. Med. Chem.* **2014**, *57*, 6275−6288.

(5) Qian, Z.; Liu, T.; Liu, Y.-Y.; Briesewitz, R.; Barrios, A. M.; Jhiang, S. M.; Pei, D. Efficient delivery of cyclic peptides into mammalian cells with short sequence motifs. *ACS Chem. Biol.* **2013**, *8*, 423−431.

(6) Qian, Z.; Dougherty, P. G.; Pei, D. Monitoring the cytosolic entry of cell-penetrating peptides using a pH-sensitive fluorophore. *Chem. Commun.* **2015**, *51*, 2162−2165.

(7) Qian, Z.; LaRochelle, J. R.; Jiang, B.; Lian, W.; Hard, R. L.; Selner, N. G.; Luechapanichkul, R.; Barrios, A. M.; Pei, D. Early endosomal escape of a cyclic cell-penetrating peptide allows effective cytosolic cargo delivery. *Biochemistry* **2014**, *53*, 4034−4046.

(8) Lian, W.; Jiang, B.; Qian, Z.; Pei, D. Cell-permeable bicyclic peptide inhibitors against intracellular proteins. *J. Am. Chem. Soc.* **2014**, *136*, 9830−9833.

(9) Jiang, B.; Pei, D. A selective, cell-permeable nonphosphorylated bicyclic peptidyl inhibitor against peptidyl-prolyl isomerase Pin1. *J. Med. Chem.* **2015**, *58*, 6306−6312.

(10) Young, A.; Lyons, J.; Miller, A. L.; Phan, V. T.; Alarcon, I. R.; McCormick, F. Ras signaling and therapies. *Adv. Cancer Res.* **2009**, *102*, 1−17.

(11) Prior, I. A.; Lewis, P. D.; Mattos, C. A. A comprehensive survey of Ras mutations in cancer. *Cancer Res.* **2012**, *72*, 2457−2467.

(12) Helwick, C. Targeting KRAS in GI Cancers: the hunt for the Holy Grail in cancer research. The ASCO Post, http://www.as-copost.com/issues/april-15-2012/targeting-kras-in-gi-cancers-the-hunt-for-the-holy-grail-in-cancer-research.aspx (2012).

(13) Russo, M.; Di Nicolantonio, F.; Bardelli, A. Climbing RAS, the Everest of oncogenes. *Cancer Discovery* **2014**, *4*, 19−21.

(14) Wang, W.; Fang, G.; Rudolph, J. Ras inhibition via direct Ras binding- is there a path forward? *Bioorg. Med. Chem. Lett.* **2012**, *22*, 5766−5776.

(15) Spiegel, J.; Cromm, P. M.; Zimmermann, G.; Grossmann, T. N.; Waldmann, H. Small-molecule modulation of Ras signaling. *Nat. Chem. Biol.* **2014**, *10*, 613−622.

(16) Stephen, A. G.; Esposito, D.; Bagni, R. K.; McCormick, F. Dragging ras back in the ring. *Cancer Cell* **2014**, *25*, 272−81.

(17) Zimmermann, G.; Papke, B.; Ismail, S.; Vartak, N.; Chandra, A.; Hoffmann, M.; Hahn, S. A.; Triola, G.; Wittinghofer, A.; Bastiaens, P. I.; Waldmann, H. Small molecule inhibition of the KRAS-PDEdelta interaction impairs oncogenic KRAS signaling. *Nature* **2013**, *497*, 638−642.

(18) Taveras, A. G.; Remiszewski, S. W.; Doll, R. J.; Cesarz, D.; Huang, E. C.; Kirschmeier, P.; Pramanik, B. N.; Snow, M. E.; Wang, Y. S.; del Rosario, J. D.; Vibulbhan, B.; Bauer, B. B.; Brown, J. E.; Carr, D.; Catino, J.; Evans, C. A.; Girijavallabhan, V.; Heimark, L.; James, L.; Liberles, S.; Nash, C.; Perkins, L.; Senior, M. M.; Tsarbopoulos, A.; Ganguly, A. K.; Aust, R.; Brown, E.; Delisle, D.; Fuhrman, S.; Hendrickson, T.; Kissinger, C.; Love, R.; Sisson, W.; Villafranca, E.; Webber, S. E. Ras oncoprotein inhibitors: the discovery of potent, Ras nucleotide exchange inhibitors and the structural determination of a drug-protein complex. *Bioorg. Med. Chem.* **1997**, *5*, 125−133.

(19) Maurer, T.; Garrenton, L. S.; Oh, A.; Pitts, K.; Anderson, D. J.; Skelton, N. J.; Fauber, B. P.; Pan, B.; Malek, S.; Stokoe, D.; Ludlam, M. J.; Bowman, K. K.; Wu, J.; Giannetti, A. M.; Starovasnik, M. A.; Mellman, I.; Jackson, P. K.; Rudolph, J.; Wang, W.; Fang, G. Small-molecule ligands bind to a distinct pocket in Ras and inhibit SOS-mediated nucleotide exchange activity. *Proc. Natl. Acad. Sci. U. S. A.* **2012**, *109*, 5299−5304.

(20) Sun, Q.; Burke, J. P.; Phan, J.; Burns, M. C.; Olejniczak, E. T.; Waterson, A. G.; Lee, T.; Rossanese, O. W.; Fesik, S. W. Discovery of small molecules that bind to K-Ras and inhibit Sos-mediated activation. *Angew. Chem., Int. Ed.* **2012**, *51*, 6140−6143.

(21) Ostrem, J. M.; Peters, U.; Sos, M. L.; Wells, J. A.; Shokat, K. M. K-Ras(G12C) inhibitors allosterically control GTP affinity and effector interactions. *Nature* **2013**, *503*, 548−551.

(22) Lim, S. M.; Westover, K. D.; Ficarro, S. B.; Harrison, R. A.; Choi, H. G.; Pacold, M. E.; Carrasco, M.; Hunter, J.; Kim, N. D.; Xie, T.; Sim, T.; Jänne, P. A.; Meyerson, M.; Marto, J. A.; Engen, J. R.; Gray, N. S. Therapeutic targeting of oncogenic K-Ras by a covalent catalytic site inhibitor. *Angew. Chem., Int. Ed.* **2014**, *53*, 199−204.

(23) Patgiri, A.; Yadav, K. K.; Arora, P. S.; Bar-Sagi, D. An orthosteric inhibitor of the Ras-Sos interaction. *Nat. Chem. Biol.* **2011**, *7*, 585−587.

(24) Leshchiner, E. S.; Parkhitko, A.; Bird, G. H.; Luccarelli, J.; Bellairs, J. A.; Escudero, S.; Opoku-Nsiah, K.; Godes, M.; Perrimon, N.; Walensky, L. D. Direct inhibition of oncogenic KRAS by hydrocarbon-stapled SOS1 helices. *Proc. Natl. Acad. Sci. U. S. A.* **2015**, *112*, 1761−1766.

(25) Hocker, H. J.; Cho, K. J.; Chen, C. Y.; Rambahal, N.; Sagineedu, S. R.; Shaari, K.; Stanslas, J.; Hancock, J. F.; Gorfe, A. A. Andrographolide derivatives inhibit guanine nucleotide exchange and abrogate oncogenic Ras function. *Proc. Natl. Acad. Sci. U. S. A.* **2013**, *110*, 10201−10206.

(26) Wu, X.; Upadhyaya, P.; Villalona-Calero, M. A.; Briesewitz, R.; Pei, D. Inhibition of Ras-effector interaction by cyclic peptides. *MedChemComm* **2013**, *4*, 378−382.

(27) Upadhyaya, P.; Qian, Z.; Habir, N. A. A.; Pei, D. Direct Ras inhibitors identified from a structurally rigidified bicyclic peptide library. *Tetrahedron* **2014**, *70*, 7714−7720.

(28) Upadhyaya, P.; Qian, Z.; Selner, N. G.; Clippinger, S. R.; Wu, Z.; Briesewitz, R.; Pei, D. Inhibition of Ras signaling by blocking Ras-effector interactions with cyclic peptides. *Angew. Chem., Int. Ed.* **2015**, *54*, 7602−7606.

(29) Waldmann, H.; Karaguni, I. M.; Carpintero, M.; Gourzoulidou, E.; Herrmann, C.; Brockmann, C.; Oschkinat, H.; Müller, O. Sulindac-derived Ras pathway inhibitors target the Ras-Raf interaction and downstream effectors in the Ras pathway. *Angew. Chem., Int. Ed.* **2004**, *43*, 454−458.

(30) Shima, F.; Yoshikawa, Y.; Ye, M.; Araki, M.; Matsumoto, S.; Liao, J.; Hu, L.; Sugimoto, T.; Ijiri, Y.; Takeda, A.; Nishiyama, Y.; Sato, C.; Muraoka, S.; Tamura, A.; Osoda, T.; Tsuda, K.; Miyakawa, T.; Fukunishi, H.; Shimada, J.; Kumasaka, T.; Yamamoto, M.; Kataoka, T. In silico discovery of small-molecule Ras inhibitors that display antitumor activity by blocking the Ras-effector interaction. *Proc. Natl. Acad. Sci. U. S. A.* **2013**, *110*, 8182−8187.

(31) Lian, W.; Upadhyaya, P.; Rhodes, C. A.; Liu, Y.; Pei, D. Screening bicyclic peptide libraries for protein−protein interaction inhibitors: discovery of a rumor necrosis factor-α antagonist. *J. Am. Chem. Soc.* **2013**, *135*, 11990−11995.

(32) Chen, X.; Tan, P. H.; Zhang, Y.; Pei, D. On-bead screening of combinatorial libraries: reduction of nonspecific binding by decreasing surface ligand density. *J. Comb. Chem.* **2009**, *11*, 604−611.

(33) Rostovtsev, V. V.; Green, L. G.; Fokin, V. V.; Sharpless, K. B. A stepwise huisgen cycloaddition process: copper(I)-catalyzed regioselective "ligation" of azides and terminal alkynes. *Angew. Chem., Int. Ed.* **2002**, *41*, 2596−2599.

(34) Tornoe, C. W.; Christensen, C.; Meldal, M. Peptidotriazoles on solid phase: [1,2,3]-triazoles by regiospecific copper(I)-catalyzed 1,3-dipolar cycloadditions of terminal alkynes to azides. *J. Org. Chem.* **2002**, *67*, 3057−3064.

(35) Liu, R.; Marik, J.; Lam, K. S. A novel peptide-based encoding system for "one-bead one-compound" peptidomimetic and small molecule combinatorial libraries. *J. Am. Chem. Soc.* **2002**, *124*, 7678−7680.

(36) Joo, S. H.; Xiao, Q.; Ling, Y.; Gopishetty, B.; Pei, D. High-throughput sequence determination of cyclic peptide library members

DOI: 10.1021/acscombsci.5b00164
ACS Comb. Sci. 2016, 18, 75−85

by partial Edman degradation/mass spectrometry. *J. Am. Chem. Soc.* **2006**, *128*, 13000−13009.
(37) Thakkar, A.; Wavreille, A.-S.; Pei, D. Traceless capping agent for peptide sequencing by partial Edman degradation and mass spectrometry. *Anal. Chem.* **2006**, *78*, 5935−5939.
(38) Pacold, M. E.; Suire, S.; Perisic, O.; Lara-Gonzalez, S.; Davis, C. T.; Walker, E. H.; Hawkins, P. T.; Stephens, L.; Eccleston, J. F.; Williams, R. L. Crystal structure and functional analysis of Ras binding to its effector phosphoinositide 3-kinase gamma. *Cell* **2000**, *103*, 931−944.
(39) Mosmann, T. Rapid colorimetric assay for cellular growth and survival: application to proliferation and cytotoxicity assays. *J. Immunol. Methods* **1983**, *65*, 55−63.
(40) Prior, I. A.; Hancock, J. F. Ras trafficking, localization and compartmentalized signaling. *Semin. Cell Dev. Biol.* **2012**, *23*, 145−153.
(41) Alessi, D. R.; James, S. R.; Downes, C. P.; Holmes, A. B.; Gaffney, P. R.; Reese, C. B.; Cohen, P. Characterization of a 3-phosphoinositide-dependent protein kinase which phosphorylates and activates protein kinase B alpha. *Curr. Biol.* **1997**, *7*, 261−269.
(42) Shelton, J. G.; Steelman, L. S.; White, E. R.; McCubrey, J. A. Synergy between PI3K/Akt and Raf/MEK/ERK pathways in IGF-1R mediated cell cycle progression and prevention of apoptosis in hematopoietic cells. *Cell Cycle* **2004**, *3*, 370−377.
(43) Sos, M. L.; Fischer, S.; Ullrich, R.; Peifer, M.; Heuckmann, J. M.; Koker, M.; Heynck, S.; Stuckrath, I.; Weiss, J.; Fischer, F.; et al. Identifying genotype-dependent efficacy of single and combined PI3K- and MAPK-pathway inhibition in cancer. *Proc. Natl. Acad. Sci. U. S. A.* **2009**, *106*, 18351−18356.
(44) Schoeberl, B.; Eichler-Jonsson, C.; Gilles, E. D.; Muller, G. Computational modeling of the dynamics of the MAP kinase cascade activated by surface and internalized EGF receptors. *Nat. Biotechnol.* **2002**, *20*, 370−375.
(45) John, J.; Sohmen, R.; Feuerstein, J.; Linke, R.; Wittinghofer, A.; Goody, R. S. Kinetics of interaction of nucleotides with nucleotide-free H-ras p2 1. *Biochemistry* **1990**, *29*, 6058−6065.
(46) Goddard-Borger, E. D.; Stick, R. V. An efficient, inexpensive and shelf-stable diazotransfer reagent: imidazole-1-sulfonyl azide hydrochloride. *Org. Lett.* **2007**, *9*, 3797−3800.

DOI: 10.1021/acscombsci.5b00164
ACS Comb. Sci. 2016, 18, 75−85